Barrón, Vidal; Méndez, José M.; Balbuena, José; Cruz-Yusta, Manuel; Sánchez, Luis; Giménez, Carmen; Sacristán, Daniel; González-Guzmán, Adrián; Sánchez-Rodríguez, Antonio R.; Skiba, Ute M.; Inda, Alberto V.; Marques, José; Recio, José M.; Delgado, Antonio; del Campillo, María C.; Torrent, José. 2020.
Photochemical emission and fixation of NOX gases in soils.

The definitive version was published in *Science of the Total Environment*, 702, 134982. 9, pp. https://doi.org/10.1016/j.scitotenv.2019.134982

Photochemical emission and fixation of NO_X gases in soils

Vidal Barrón[a,*], José M. Méndez[a], José Balbuena[b], Manuel Cruz-Yusta[b], Luis Sánchez[b], Carmen Giménez [a], Daniel Sacristán[a], Adrián González-Guzmán[a], Antonio R. Sánchez-Rodríguez[a,c], Ute M. Skiba[d], Alberto V. Inda[e], José Marqués[f], José M. Recio[g], Antonio Delgado[h], María C. del Campillo[a], José Torrent[a]

[a] Departamento de Agronomía, Universidad de Córdoba, 14071 Córdoba, Spain

[b] Departamento de Química Inorgánica e Ingeniería Química, Instituto Universitario de Investigación en Química Fina y Nanoquímica, Universidad de Córdoba, 14071 Córdoba, Spain.

[c] School of Natural Sciences, Environment Centre Wales, Bangor, Gwynedd LL57 2UW, United Kingdom.

[d] Centre for Ecology and Hydrology (CEH), Edinburgh, Bush Estate, Penicuik, Midlothian EH260QB, United Kingdom.

[e] Departamento de Solos, Universidade Federal do Rio Grande do Sul, 90040-060, Porto Alegre, Brazil.

[f] Departamento de Solos e Adubos, Faculdade de Ciências Agrárias e Veterinárias de Jaboticabal, UNESP – Universidade Estadual Paulista, 14884-900, Jaboticabal, Brazil.

[g] Departamento de Botánica, Ecología y Fisiología Vegetal, Facultad de Ciencias, Universidad de Córdoba, 14071 Córdoba, Spain.

[h] Departamento de Ciencias Agroforestales, ETSIA, Universidad de Sevilla, 41013 Sevilla, Spain

*Corresponding author. Email: vidal@uco.es

***Graphical Abstract**

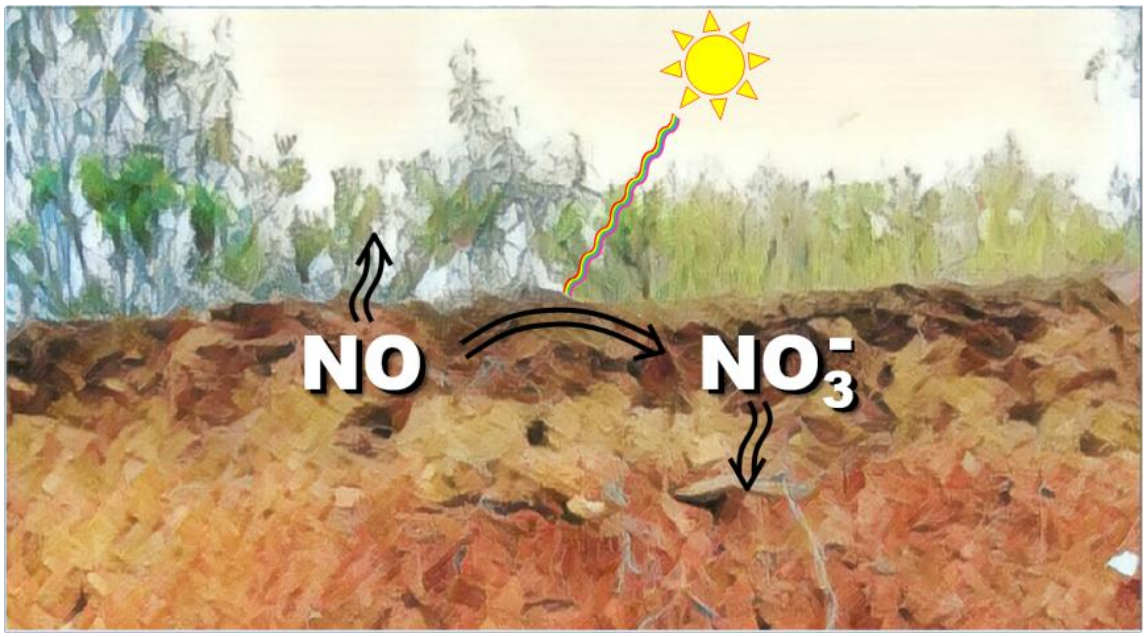

ABSTRACT

Gaseous nitrogen oxides (NOx), which result from the combustion of fossil fuels, volcanic eruptions, forest fires, and biological reactions in soils, not only affect air quality and the atmospheric concentration of ozone, but also contribute to global warming and acid rain. Soil NOx emissions have been largely ascribed to soil microbiological processes; but there is no proof of abiotic catalytic activity affecting soil NO emissions. We provide evidence of gas exchange in soils involving emissions of NOx by photochemical reactions, and their counterpart fixation through photocatalytic reactions under UV–visible irradiation. The catalytic activity promoting NOx capture as nitrate varied widely amongst different soil types, from low in quartzitic sandy soils to high in iron oxide and TiO_2 rich soils. Clay soils with significant amounts of smectite also exhibited high rates of NOx sequestration and fixed amounts of N comparable to that of NO (nitric oxide) losses through biotic reactions. In these soils, a flux of 100 μg N_{NO} m^{-2} h^{-1}, as usually found in most ecosystems, could be reduced by these photochemical reactions by more than 60%. This mechanism of N fixation provides new insight into the nitrogen cycle and may inspire alternative strategies to reduce NO emissions from soils.

Keywords: NOx, nitric oxide, nitrogen cycle, soil photocatalysis.

1. Introduction

Gaseous NO (nitric oxide) and NO_2 (nitrogen dioxide), which are collectively termed NOx, are well known as air pollutants because they accumulate in large cities, mainly by combustion of fossil fuels. In addition, NOx originates from volcanic eruptions, lightning strikes, forest fires (Manahan, 2009) and soil biotic nitrification and denitrification (Butterbach-Bahl et al., 2011; Pilegaard, 2013; Medinets et al., 2015; Sanz-Cobena et al., 2017). In high concentrations, NOx is harmful to human health, animals and plants, contributes to the formation of smog, acid rain and is relevant in the chemistry of tropospheric ozone and that of gases with a strong greenhouse effect such as N_2O (Crutzen, 1979).

Photocatalytic oxidation is an especially simple and effective NOx decontamination (De-NOx) strategy based on the photocatalytic properties of certain semiconductor materials capable of promoting NOx oxidation with the help of oxygen, water and light (Balbuena et al., 2015). The reaction involves activation of the semiconductor surface by light with energy similar to or greater than that of the band gap, transferring electrons from the valence band to the conduction band and creating electron–hole pairs. Both photogenerated electrons and holes can react with water and oxygen to form reactive oxygen species (ROS) such as $^{\bullet}O_2^-$ and $^{\bullet}OH$ radicals that transform NOx into nitrate (NO_3^-) (Balbuena et al., 2015). The semiconductor materials used for this purpose are mainly synthetic compounds such as TiO_2, of which the anatase phase is the most effective De-NOx photocatalyst, α-Fe_2O_3 and ZnO, either alone or in combination with additives such as clay, carbon or mesoporous materials (Balbuena et al., 2015; Sugráñez et al. 2015). Moreover, some of these efficient photocatalytic materials occur naturally in soil.

Soils also contribute to NOx production through microbial nitrification and denitrification, and abiotic chemodenitrification, having a strong impact on the N cycle in soils (Firestone and Davidson, 1989; Butterbach-Bahl et al., 2011; Pilegaard, 2013; Ábalos et al., 2014; Medinets et

al., 2015; Sanz-Cobena et al., 2017; Yao et al., 2019). In fact, such processes reduce the plant available N, which in agricultural soils comes mostly from industrially produced mineral N fertilizers. The manufacture of these fertilizers through the Haber-Bosch process is very energy demanding, and is among the main contributors to agriculturally related CO_2 emissions. The majority of the mechanisms involved in the emission of NO, N_2O and N_2 gases, and the biological and industrial fixation of N_2, have been investigated for more than 100 years (Keeney and Hatfield, 2008). A plethora of studies have addressed the factors governing the complex balance of N gases in soils, including vegetation, microorganisms, organic matter, N availability, oxygen status and soil moisture, pH and temperature, in addition to soil fertilization and management in agricultural systems. This deep knowledge facilitates the estimation of gaseous N emissions (Cowan et al., 2019) and is used to improve agroecosystem management. To the authors' knowledge, however, no study to date has focused on NOx fixation reactions in soils, mediated by the specific effect of light, or on their relevance to the soil N cycle, and hence on the exchange of gases between terrestrial ecosystems and the atmosphere. Recently, Doane et al. (2019) reported significant alterations of several soil chemical properties by the effect of light. In other papers, Doane (2017a,b; and references therein) also reviewed the considerable list of photochemical reactions known in natural media. Nevertheless, this author recognizes a knowledge gap about the photochemical reactions related to abiotic N in soils and emphasizes that photochemical N fixation could be more than negligible and points out the necessity for research in this field. More recently, the "photoelectric device" of Fe oxyhydroxides mineral coatings involved in the redox chemistry on Earth´s surface has also been reported (Lu et al., 2019).

Based on the photochemical properties of some compounds present in soils, it can be hypothesized that they may contribute to nitrification and denitrification processes. To assess

this, we performed a pioneering study of light induced chemical reactions of NO with six soils differing in colour, particle size distribution, organic matter content and mineralogy.

2. Materials and Methods

2.1. Soil sample location

Details of sample collection are available in Table S1 (Supplementary data).

2.2. Mineralogical and chemical analysis of soils

The soil samples were air-dried, sieved to 2 mm and analyzed for particle size distribution with the pipette method (Gee and Bauder, 1986), pH in a 1:2.5 soil:water ratio, hygroscopic water with the oven-dry test at 110 ºC and organic matter with the Walkley–Black method (Nelson and Sommers, 1982). Mineral phases were identified and quantified by (a) X-ray diffraction (XRD) (Whiting and Allardice, 1986) on a Bruker D8 Advance instrument using Cu Kα radiation (Fig. S1; Supplementary Data) and (b) elemental chemical analysis after microwave assisted digestion of 50 mg of soil sample with a mixture of concentrated reagents containing 2 mL H_2O_2, 1 mL HF, 3 mL HNO_3 and 0.5 mL HCl in a Milestone Ultrawave oven. Then, the main elements were quantified by ICP-MS on a Perkin Elmer NexION350X spectrometer. Hematite and goethite were quantitatively estimated from the visible spectra of pressed fine powders (Torrent and Barrón, 2008) which were recorded on a Cary 5000 spectrophotometer equipped with a diffuse reflectance accessory (Fig. S2; Supplementary Data). The specific surface area was determined by N_2 adsorption (BET method) on a Micromeritics ASAP 2020 instrument and microporosity was determined with the t-plot method (Gregg and Sing, 1982). Samples for soil N analysis were extracted with 0.5 M K_2SO_4 at a soil:solution ratio of 1:2. Nitrate and ammonium (NH_4^+) were measured by spectrophotometry on a Power-Wave-XS microplate reader according to the methods proposed by Miranda et al. (2001) and Mulvaney et

al.(1996), respectively, and total dissolved nitrogen, TDN, with a Multi N/C 2100/2100 analyzer (Analytik Jena AG, Jena, Germany). Soluble organic nitrogen (SON) was calculated by subtracting NO_3^- and NH_4^+ from TDN.

2.3. Photochemical experiments

The photocatalytic activity of the materials towards the oxidation of NO was assessed by using a 25 cm^2 sample holder placed in a laminar flow reactor (Fig.S3; Supplementary data). A 5 g soil sample was used in each photocatalytic run. Artificial sunlight from a Solarbox 3000e RH with UV and visible irradiance of 25 and 550 W m^{-2}, respectively, was used for most of the experiments. Furthermore, two lower irradiances were used to evaluate the light intensity effect: 20 (UV) and 375 (Vis), and 13.5 (UV) and 250 (Vis) Wm^{-2}. The concentrations of NO and NO_2 were accurately measured with an Environment AC32M chemiluminescence analyser. The photoreactor was fed with a mixture of air and NO, and the two streams were mixed to obtain the desired NO concentration. The air was passed through a bottle filled with demineralized water to maintain a constant relative humidity of 50 ± 5% of the supplied gas. A flow rate of 0.30 L min^{-1} was used. Passing the air/NO gas stream over the sample in the dark for 10 min caused no change in the NO concentration profiles, thus ruling out potential NO adsorption onto the sample surface or its direct photolysis. Subsequently, the photoreactor was irradiated for 180 min.

Photocatalytic experiments were carried out using three replicates for each of the six soils. The four treatments were: 1) control ("C"), no treatment, except zero air (N_2 + O_2) during the photochemical test. The other experiments were performed under a NO concentration of 100 ppb: on 2) natural ("N") and 3) organic matter-free ("O") soils. The "O" soils were treated with H_2O_2, washed four times with 0.5 M K_2SO_4 and twice with deionized water, sterilized by autoclaving for 25 min twice with an interval of 24 hours, and then freeze-dried; the last group

was 4) washed ("W") four times with 0.5 M K_2SO_4 and twice with deionized water and then freeze-dried.

2.4. Statistical analysis

Analyses of variance were performed for ΣNOx (all soils) and for NO conversion (FLU and CAL) using Statistix v.9 software. Means were separated via the least significant difference (LSD) test (p<0.05). Principal component analysis (PCA) was performed to explore the relationships between NOx gases (emitted or fixed) and the remaining soil variables analysed for the six soils used in our experiments, based on a data correlation matrix (SPSS v25.0; IBM Corp., Armonk, NY).

3. Results

3.1. Soil Properties

Soil samples varied widely in mineral composition (Table 1), consistent with their different parent materials (Table S1; Supplementary Data). Quartz was almost the only mineral in the sandy dune soil (Arenosol, *ARE*) and one of the most abundant minerals in the rest of the samples. Feldspar and mica completed the sandy fraction in some soils. Among the silicate clay minerals, illite was the main phase except in the highly weathered tropical soil (Ferralsol, *FER*), rich in kaolinite. In the calcareous soil (Calcisol, *CAL*), a significant proportion of smectite was present. Poorly crystalline silicate minerals were an important component in the Andisol (*AND*). The proportion of iron oxides as hematite (α-Fe_2O_3) ranged from 0 to 28% (for the red Ferralsol, *FER*) and goethite (α-FeOOH) was also present in some soils. TiO_2 appeared in all samples at low concentrations (<1%) except in the Ferralsol (4%), where the anatase phase could be identified. Calcite was present in a notable amount in the alluvial soil (Fluvisol, *FLU*) and,

169 especially, in the soil developed from calcareous materials (Calcisol, *CAL*). The particle size
170 distribution ranged widely from sandy (*ARE, CAM, AND* and *FLU*) to clayey soils (*FER*, *CAL*).
171 Consequently, the surface area reached a value of 38.5 m^2g^{-1} for the clayey Ferralsol (*FER*) and a
172 high microporosity (pore diameter < 2 nm) was found in the smectitic sample (*CAL*). Organic
173 matter ranged from close to 0% in the Arenosol (*ARE*) to 2.1 and 8.3% in the Cambisol (CAM)
174 and the forest Andisol (*AND*), respectively. Consistent with these data the latter soils exhibited a
175 significantly higher concentration of NO_3^-, probably as a product of organic matter
176 mineralization.

177

178 *3.2. Photochemical reactions of NOx in soils*

179 A marked decrease in NO concentration (blue line, Fig. 1) in the gas flow through
180 irradiated raw samples (N treatment) was observed in four (*ARE, FLU, FER,* and *CAL*) of the six
181 soils. This reveals NO fixation, which ranged from low levels in the sandy soil (*ARE*) up to more
182 than half of the initial NO concentration supplied (e.g., in *CAL*, where the initial 100 ppb was
183 reduced by an average of 53.5%). The shape of the NO curves varied amongst the different soil
184 samples. This may be ascribed to the differences in gas diffusion associated with different soil
185 particle size distributions and porosity. A contrasting effect, i.e., emission of NO under
186 irradiation, was found in two of the studied samples (*CAM* and *AND*), corresponding to soils
187 with high organic matter content and high soluble NO_3^- concentrations.

188 After removing the organic matter with H_2O_2 (O treatment) the NOx curves became
189 similar to those of the previously studied samples (Fig. S4; Supplementary Data). This reveals
190 photochemical fixation of NO after organic matter removal. Washing the soils with de-ionized
191 water plus K_2SO_4 (W treatment) produced a similar effect, suggesting that the emission of NO
192 was a product of the photochemical oxidation of soluble NO_3^- (Fig. S5; Supplementary Data).

For soils irradiated in the presence of N_2 but not NO (control, C treatment), a low emission of NOx was exhibited by *ARE, FLU, FER* and *CAL*, whereas a high emission (comparable to that of the experiment with NO) was observed for higher organic matter soils, such as *CAM* and *AND* (Fig. S6; Supplementary Data).

These changes could be quantitatively evaluated from the cumulative amount of NOx removed from the gas flow (ΣNOx from Fig.1 and Figs. S4, S5, S6; Supplementary Data). Positive ΣNOx (yellow areas) indicated NOx fixation while negative ΣNOx (blue areas) denoted NOx emission. In general, for the first four soils (*ARE, FLU, FER* and *CAL*), there was low NO emission for the control treatment, however, the other three treatments (N, O and W) produced the opposite effect (NOx fixation) according to the ΣNOx (Fig. 2). This effect was significant ($p< 0.05$) for these three treatments in the *FLU, FER* and *CAL* soils when compared to the control but only for the O treatment in the *ARE* soil. In the *CAL* soil, NO fixation increased significantly in the order C<W<O<N. For the soils with the highest organic matter and NO_3^- contents (*CAM* and *AND*), there was a high NO emission in the N and C treatments (Fig. 2 and Fig. S6; Supplementary Data). After removing organic matter (O) or washing the soil (W) the effect was similar to that exhibited by the other four soils (NO fixation, Fig. 2 and Fig. S4 and S5; Supplementary Data).

The PCA of the ΣNOx gases, soil components and soil properties explained 96.7% of the total variance of our data (the first principal component or PC1 accounted for 34.8%, the PC2 for 27.5%, the PC3 explained 22.1% and the PC4 12.3%). Fig. S7 (Supplementary Data) shows the effect of removing soluble salts ("W" treatment) and organic matter ("O" treatment) on ΣNOx emissions from the soil samples, using PC1 VS. PC3. ΣNOx emission for the soil samples in which organic matter was removed were more related to surface area and the goethite, TiO_2,

clay, hematite, kaolinite and gibbsite contents, than that from the untreated soil samples (Fig. S7; Supplementary data).

The decrease of NO concentrations corresponds to the $NO \rightarrow NO_2 \rightarrow NO_3^-$ photochemical oxidation process (Balbuena et al., 2015). The negligible increase of NO_2 (black line in Fig. 1) in most cases, suggests an almost complete N fixation as NO_3^-. This was confirmed by the chemical analysis for NO_3^- in the soils after irradiation. A balance of the transformation from NOx to NO_3^-(details of the stoichiometric calculations in Supplementary data) was performed for the O and W treatments because in these samples most indigenous NO_3^- was previously removed. As shown in Table 2, the measured $NO_3^-$was 6.4 to 25.1 times that estimated from the stoichiometric calculations.

3.3. Effect of NO concentration and light intensity

A lower initial NO concentration (below 50 ppb) yielded a significantly higher percentage of conversion of NO under irradiation for the FLU and CAL soils (Fig. 3A). Similar behaviour has also been observed in the photocatalytic oxidation of NO passed over a TiO_2 catalyst (Devahasdin et al., 2003). As NO conversion is limited by the amount of NO adsorbed on the active sites, a high proportion of the gas molecules is adsorbed at the lowest initial concentration, thus increasing the efficiency of the conversion process.

According to our experimental conditions (see method section), a NO concentration of 20 ppb corresponded to a NO flux of 90 $\mu g\ N_{NO}\ m^{-2}\ h^{-1}$ (see calculations in Supplementary data). Therefore, for emission rates less than 100 $\mu g\ N_{NO}\ m^{-2}\ h^{-1}$, as is usually found in most ecosystems (Ludwig et al., 2001), the percentage of NO fixation caused by photochemical mechanism could reach, in some soils, conversion values higher than 60%. The decreasing trend in the fraction of

converted NO seems to be above 50 ppb NO, equivalent to a flux of 225 μg $N_{NO}\,m^{-2}\,h^{-1}$, a value comparable to the NO concentration in some urban environments (Balbuena et al., 2015) and below the maximum emission of NO detected in heavily fertilized soils (Almaraz et al., 2018).

Although no significant effect of light intensity was detected (Fig. 3B), a small increase in the mean values of NO conversion was observed for the highest light intensities.

4. Discussion

No previous references have been found about similar results using authentic soils; therefore, the following discussion will be based on the well-known photocatalytic properties of some minerals. Titanium and iron oxides, present in all of the studied soils, are semiconductors (SC) with proven photocatalytic activity. The photocatalytic mechanism affording complete oxidation of NO to NO_3^- or nitric acid (HNO_3) is a complex process involving several intermediate species (Balbuena et al., 2015). Basically, the process comprises several one-electron transfer steps, with nitrous acid (HONO) and nitrogen dioxide (NO_2) as intermediates (Bloh et al., 2014). Irradiating the semiconductor metal oxide particles with sunlight (Fig. S8; Supplementary Data) causes an electron in the valence band (VB) to acquire the energy of a photon and become a photo-generated electron (e^-) that migrates to the conduction band (CB) while leaving a photo-generated hole (h^+) behind as shown in Reaction [1] (Chen et al., 2012).

$$SC + h\nu \rightarrow e^- + h^+ \qquad [1]$$

The ensuing pair of mobile charges can reach the surface of the semiconductor particles and, in contact with oxygen and water molecules (Reactions [2] and [3]), assist the formation of reactive oxygen species (ROS) to initiate the progressive oxidation of NO (Chen et al., 2012).

$$O_2^- + e^- \rightarrow {}^{\bullet}O_2^- \qquad [2]$$

$$H_2O + h^+ \rightarrow H^+ + {}^{\bullet}OH \quad [3]$$

The formed hydroxyl radicals ($^{\bullet}OH$) oxidize NO to NO_2, which in turn produces nitrite (NO_2^-) and NO_3^- ions through Reactions [4] to [7].

$$NO + 2\ {}^{\bullet}OH \rightarrow NO_2 + H_2O \quad [4]$$

$$NO + NO_2 + H_2O \rightarrow 2\ HNO_2 \quad [5]$$

$$HNO_2 + {}^{\bullet}OH \rightarrow NO_2 + H_2O \quad [6]$$

$$NO_2 + {}^{\bullet}OH \rightarrow NO_3^- + H^+ \quad [7]$$

On the other hand, a superoxide radical takes part in the final oxidation of nitrogen oxide gases to NO_3^- ions (Reactions [8] and [9]) (Chen et al., 2012; Balbuena et al., 2015).

$$NO + {}^{\bullet}O_2^- \rightarrow NO_3^- \quad [8]$$

$$NO_2 + \tfrac{1}{2}\ {}^{\bullet}O_2^- \rightarrow NO_3^- \quad [9]$$

Photons in UV solar light can supply enough energy to overcome the TiO_2 band gap (3.2 eV for the anatase phase). Conversely, the small band gap of hematite (1.9–2.2 eV) can be overcome with photons in the visible light range of the solar spectrum (Fig. S8; Supplementary Data). Consistent with this mechanism, *FER* (Ferralsol), which is the soil with the highest amounts of Fe oxides, exhibited a high NO conversion. This result suggests that the assumed chemical synergy between Fe_2O_3/TiO_2 semiconductors for synthetic materials (Balbuena et al., 2016) is echoed by soils. Although most soils contained only small amounts of Ti and Fe oxides, the observed activity agrees with the catalytic activity found in aerosols with low concentrations of these oxides (George et al. 2015).

The strong catalytic effect of the CAL soil sample (Calcisol) may be ascribed to the presence of other minerals, such as smectite, which was measured in significant amount only in this soil. Smectite is known to produce ROS species via photocatalytic reactions (Yuan et al., 2016).Tests conducted in parallel with pure minerals (Fig. S9; Supplementary Data) also revealed catalytic ability in silicate minerals such as feldspar, mica and smectite, which proved to be similarly efficient to α-Fe_2O_3, ZnO and TiO_2 in decreasing NOx levels. On the other hand, smectite was successfully used as a catalyst support to disperse titanium (anatase) and titanium–iron species to produce a photocatalyst with proved activity (Carriazo et al., 2010). Its presence in the CAL soil influenced the particle size distribution and surface area (Table 1), —in fact, a microporosity of 59.5% was measured. The different soil pore space can alter the gas diffusion as a result, making active reaction sites more readily accessible to the reactant molecules and increasing reactivity as a result. Moreover, the good dispersion of the main active semiconductors (TiO_2 and α-Fe_2O_3) allowed for better light harvesting. Thus, in comparison with FLU soil, exhibiting only small changes in NO conversion with the light intensity (Fig. 3B), the NO conversion significantly increased when the CAL soil was irradiated with the highest irradiance.

We found that the amount of NO_3^- formed was an order of magnitude greater than that coming from the fixed NOx, i.e., from the amount that disappeared from the gas flux during the photocatalytic experiment. This suggests that not only was NO photocatalytically-oxidized but also nitrogen gas, N_2, which was the carrier for NO in our experiment, was also photocatalytically oxidized. Nitrogen gas, therefore, could also contribute to the increase of NO_3^- in the tested soils. This was also suggested by Medford and Hatzell (2017), who reported the small but credible scientific evidence for nitrogen gas fixation by photochemical processes, in particular, based on Yuan et al. (2013) observing photocatalytic formation of NO_3^- from

306 atmospheric nitrogen. According to these authors, the following photocatalytic reactions
307 proposed for TiO_2 could also be involved in our soils:

308 $N_2 + O_2 \rightarrow 2NO$ [10]

309 $N_2 + 2H_2O + 4\ h^+ \rightarrow 4\ H^+ + 2NO$ [11]

310 Therefore, the NO produced on the soil surface could follow the above-mentioned
311 reactions [4-9].

312 The emission of NO by soils has largely been ascribed to biological nitrification and
313 denitrification processes (Butterbach-Bahl et al., 2011; Pilegaard, 2013; Medinets et al., 2015;
314 Sanz-Cobena et al., 2017), but only in selected cases, such as in desert soils, has abiotic nitrogen
315 loss at high temperature driven by solar radiation been reported (McCalley and Sparks,
316 2009).We have shown here that light can also trigger NO and NO_2 emission in other soils (Fig.
317 1, *CAM* and *AND*) with a net emission of NOx upon irradiation, i.e., although the photocatalytic
318 fixation may have also occurred, the balance was a net emission of NOx. This may be due to
319 photochemical decomposition of adsorbed NO_3^- (Ndour et al., 2009; Nanayakkara et al., 2014;
320 George et al., 2015) present in substantial amounts in these soils. As reported, in the review by
321 George et al. (2015) two pathways from NO_3^- to NOx are possible:
322 1) *Photocatalysis-Photolysis*: adsorbed NO_3^- on the soil surface (SS) can react with the holes
323 (h^+), previously generated by interaction with photons ($h\nu$). Therefore, NO_3^- radicals ($NO_3^\bullet$) can
324 be formed and subsequently reduced to NO and NO_2 by photolysis, through the following
325 reactions:

326 $SS + h\nu \rightarrow e^- + h^+$ [12]

327 $NO_3^- + h^+ \rightarrow NO_3^\bullet$ [13]

328 $NO_3^\bullet + h\nu \rightarrow NO + O_2$ [14]

$$NO_3^{\bullet} + h\nu \rightarrow NO_2 + O^{\bullet} \quad [15]$$

2) *Photolysis*: aqueous NO_3^- can absorb light transforming itself into NO_2 and NO gases, through the following reactions:

$$NO_3^- + h\nu \rightarrow NO_2 + O^{\bullet -} \quad [16]$$

$$NO_3^- + h\nu \rightarrow NO_2^- + O^{\bullet}(^3P) \quad [17]$$

$$O^{\bullet -} + H_2O \rightarrow OH^{\bullet} + OH^- \quad [18]$$

$$NO_2^- + h\nu \rightarrow NO + O^- \quad [19]$$

This second mechanism has been reported to explain the NOx contribution from snow and ice in polar regions (Grannas et al., 2007).

The presence of photocatalytic surfaces in our soils and the dominant emission of NO versus NO_2 (see Fig. 2 for CAM and AND soils) make the first mechanism (photocatalysis-photolysis) more plausible.

Any of these mechanisms could also be responsible for the initial sharp decrease in NOx, observed in all cases where NOx fixation occurs, and can later be balanced by the conversion of NO_3^- to NOx. These processes may be responsible for the lack of a continuous increase in the amount of fixed NO_3^- not to continuously increase in nature.

Other potential mechanisms may also explain the emission of NOx gases:

3) *Organic N photodegradation:* chromophores in some organic compounds can absorb light and subsequently promote the decomposition of soil organic N compounds into NOx gases (Katagi, 2004; Austin and Vivanco, 2006; Georgiou et al., 2015). According to Gohre et al.(1986), indirect photo-oxidation of organic substances can produce ROS, such as singlet oxygen. Furthermore, a previous reaction (equation [18]) driving the formation of highly reactive radical $OH^{\bullet}$ can also contribute to an easier photo-degradation of organic N.

352 Overall, the removal of organic matter led to no emission but fixation of NOx in the tested
353 soils (Fig. S4 and Fig. 2, *CAM-O* and *AND-O*). A similar effect was observed for the washed
354 samples (Fig. S5 and Fig. 2, *CAM-W* and *AND-W*), which suggests that NO_3^- might be the
355 preferentially photodegraded fraction.

356 Our results reveal that a non-negligible phenomenon in the nitrogen cycle "puzzle" could
357 be missing (Fig.4). Photochemical reactions on soil surfaces should be considered to draw a
358 more complete view of the N cycle in soils and in nature. Abiotic fixation of NOx may be
359 relevant in soils containing photocatalytic minerals capable of producing ROS. These
360 compounds can oxidize NOx gases eventually released from soils through biotic nitrification,
361 denitrification or organic matter degradation to NO_3^-. What is observed in soils is the resulting
362 balance of several processes in which this photocatalytic reaction is involved. In this way, a
363 natural mechanism would contribute to decreasing the adverse effects of NO and maintaining
364 adequate levels of plant available N in soil.

365 These mechanisms might be important in soils containing substantial amounts of smectite
366 and, also, in many tropical and subtropical soils, where iron and Ti oxides are relatively
367 abundant (Cornell and Schwertmann, 2003). Additionally, they may somehow govern the
368 atmospheric N composition of planet Mars, whose surface is rich in such minerals (Chevrier and
369 Mathe, 2007).We can also tentatively hypothesize that this photocatalytic mechanism could
370 explain the high levels of NO_3^- found on the surface of Mars (Stern et al., 2015), where no
371 biological activity is present.

372

373 **5. Conclusions**

374 In summary, light exposure induced a photochemical pathway for N gas exchange from
375 soils. This is a complex process influenced by the overall mineralogical composition

(particularly by minerals with potential photocatalytic activity), microstructure, organic carbon and water content. Obviously, further research via laboratory experiments and field trials is necessary to ascertain the actual scope of this new finding. Some widely recognized uncertainties in emission models for NOx in soils (Davidson et al., 2000; Hutchinson et al., 1997) could be solved by considering this process. It is also worth noting that our research suggests that light (especially in the UV region) can significantly influence NO emission measurements. Consequently, it is advisable that the typically opaque chambers for gas measurements should be redesigned for allowing natural light to pass. This implies the use of quartz rather than glass or methacrylate windows, given that the latter absorb a substantial part of UV light.

On the other hand, it has been also shown (Homyak et al., 2016) that reduced rainfall and increased drought periods, predicted by climate models for some regions, could trigger unexpected NO emissions, therefore increasing the future relevance of this gas. Finally, this study may inspire new soil and fertilizer management practices aimed at reducing N losses and, probably, new tools to mitigate NOx pollution in urban areas.

Acknowledgments

This work was funded by Spain's Ministry of Economy and Competitiveness (Project AGL 2017-87074-C2-2-R and MAT2017-88284-P), Junta de Andalucía (Group FQM-175), the University of Córdoba (Project 20 Plan Propio Modalidad 4.1) and the European Regional Development Fund. We thank the Servicio Central de Apoyo a la Investigación (SCAI) and the Fine Chemistry and Nanochemistry Research Institute (IUI-QFN) of the University of Córdoba for technical support in the conducting of the elemental chemical and physical analyses, respectively. Constructive comments by reviewers are highly appreciated.

Appendix A. Supplementary Data.

See attached file

References

Ábalos, D., Sánchez-Martín, L., García-Torres, L., van Groenigen, J.W., Vallejo, A., 2014. Management of irrigation frequency and nitrogen fertilization to mitigate GHG and NO emissions from drip-fertigated crops. Sci. Total Environ. 490, 880–888. DOI: 10.1016/j.scitotenv.2014.05.065. Epub 2014 Jun 5.

Almaraz, M., Bai, E., Wang, C., Trousdell, J., Conley, S., Faloona, I., Houlton, B.Z., 2018. Agriculture is a major source of NOx pollution in California. Sci. Adv. 4, eaao3477. DOI: 10.1126/sciadv.aao3477.

Austin, A.T., Vivanco, L., 2006. Plant litter decomposition in a semi-arid ecosystem controlled by photodegradation. Nature 442, 555–558. DOI:10.1038/nature05038.

Balbuena, J., Carraro, G., Cruz-Yusta, M., Gasparotto, A., Maccato, C., Pastor, A., Sada, C., Barreca, D., Sánchez, L., 2016. Advances in photocatalytic NOx abatement through the use of Fe_2O_3/TiO_2 nanocomposites. RSC Adv. 6, 74878–74885. DOI: 10.1039/c6ra15958c.

Balbuena, J., Cruz-Yusta, M., Sánchez, L., 2015. Nanomaterials to combat NOx pollution. J. Nanosci. Nanotechnol. 15, 6373–6385. DOI:10.1166/jnn.2015.10871.

Bloh, J.Z., Folli, A., Macphee, D.E., 2014. Photocatalytic NOx abatement: Why the selectivity matters. RSC Adv. 4, 45726–45734. DOI:10.1039/C4RA07916G.

421 Butterbach-Bahl, K., Gundersen, P., Ambus, P., Augustin, J., Beier, C., Boeckx, P.,
422 Dannenmann, M., Sánchez-Gimeno, B., Kiese, R., Kitzler, B., Ibrom, A., Rees, R.M., Smith,
423 K.A., Stevens, C., Vesala, T., Zechmeister-Boltenstern, S., 2011. Nitrogen processes in
424 terrestrial ecosystems. In: The European Nitrogen Assessment (Eds. M.A. Sutton et al.)
425 Cambridge University Press, Cambridge. pp. 99–125.
426 DOI:10.1017/CBO9780511976988.009.

427 Carriazo, J.G., Moreno-Forero, M., Molina, R.A., Moreno, S., 2010. Incorporation of titanium
428 and titanium–iron species inside a smectite-type mineral for photocatalysis. Appl. Clay Sci.
429 50, 401–408. https://doi.org/10.1016/j.clay.2010.09.007.

430 Chen, H., Nanayakkara, C.E., Grassian, V.H., 2012. Titanium dioxide photocatalysis in
431 atmospheric chemistry. Chem. Rev. 112, 5919–5948. DOI: 10.1021/cr3002092.

432 Chevrier, V., Mathe, P., 2007. Mineralogy and evolution of the surface of Mars: A review.
433 Planet. Space Sci. 55, 289–314. DOI: 10.1016/j.pss.2006.05.039.

434 Cornell, R.M., Schwertmann, U., 2003. The iron oxides: Structure, properties, reactions,
435 occurrences and Uses, Wiley–VCH, Weinheim. pp. 433–468. DOI:10.1002/3527602097.

436 Cowan, N., Levy, P., Drewer, J., Carswell, A., Shaw, R., Simmons, I., Bache, C., Marinheiro, J.,
437 Brichet, J., Sánchez-Rodríguez, A.R., Cotton, J., Hill, P., Chadwick, D.R., Jones, D.L.,
438 Misselbrook, T.H., Skiba, U., 2019. Environ. Int. 128, 362–370.
439 DOI:10.1016/j.envint.2019.04.054.

440 Crutzen, P.J., 1979. The Role of NO and NO_2 in the Chemistry of the Troposphere and
441 Stratosphere. Annu. Rev. Earth Planet. Sci.7, 443–472.
442 DOI:10.1146/annurev.ea.07.050179.002303.

443 Davidson, E.A., Keller, M., Erickson, H.E., Verchot, L.V., Veldkamp, E., 2000. Testing a
444 conceptual model of soil emissions of nitrous and nitric oxides. Bioscience 50, 667–680.
445 DOI:10.1641/0006-3568(2000)050[0667:TACMOS]2.0.CO;2.

446 Devahasdin, S., Fan, Jr. C., Li, K., Chen, D.H., 2003. TiO_2 photocatalytic oxidation of nitric
447 oxide: transient behavior and reaction kinetics. J. Photochem. Photobiol. A156, 161–170.
448 DOI: 10.1016/S1010-6030(03)00005-4.

449 Doane, T.A., 2017a. A survey of photogeochemistry. Geochem. Trans. 18, 1. DOI:

450 10.1186/s12932-017-0039-y.

451 Doane, T.A., 2017b. The Abiotic Nitrogen Cycle. ACS Earth Space Chem. 1, 411–421. DOI:
452 10.1021/acsearthspacechem.7b00059.

453 Doane, T.A., Silva, L.C.R., Horwath, W.R., 2019. Exposure to Light Elicits a Spectrum of
454 Chemical Changes in Soil. J. Geophys. Res-Earth 124, 2288–2310.
455 DOI:10.1029/2019JF005069.

456 Firestone, M.K., Davidson, E.A. 1989. Microbiological basis of NO and N_2O production and
457 consumption in soil. In: Exchange of trace gases between terrestrial ecosystems and the
458 atmosphere (Eds. M.O. Andreae, D.S. Schimel). John Wiley & Sons, New York. pp. 7–21.
459 WOS:A1989BU45V00002.

460 Gee, G.W., Bauder, J.W., 1986. Particle size analysis. In: Methods of soil analysis. Part 1.
461 Physical and mineralogical methods (Ed. A. Klute). American Society of Agronomy, Soil
462 Science Society of America, Madison. pp 383–411. DOI: 10.2136/sssabookser5.1.2ed.c15.

463 George, C., Ammann, M., D'Anna, B., Donaldson, D.J., Nizkorodov, S.A., 2015. Heterogeneous
464 photochemistry in the atmosphere. Chem. Rev. 115, 4218–4258. DOI: 10.1021/cr500648z.

Georgiou, C.D., Sun, H.J., McKay, C.P., Grintzalis, K., Papapostolou, I., Zisimopoulos, D., Panagiotidis, K., Zhang, G., Koutsopoulou, E., Christidis, G.E., Margiolaki, I., 2015. Evidence for photochemical production of reactive oxygen species in desert soils. Nat. Commun. 6, 7100. DOI: 10.1038/ncomms8100.

Gohre, K., Scholl, R., Miller, G.C., 1986. Singlet oxygen reactions on irradiated soil surfaces. Environ. Sci. Technol. 20, 934–938. DOI: 10.1021/es00151a013.

Grannas, A.M., Jones, A.E., Dibb, J., Ammann, M., Anastasio, C., Beine, H.J., Bergin, M., Bottenheim, J., Boxe, C.S., Carver, G., Chen, G., Crawford, J.H., Dominé, F., Frey, M.M., Guzmán, M.I., Heard, D.E., Helmig, D., Hoffmann, M.R., Honrath, R.E., Huey, L.G., Hutterli, M., Jacobi, H.W., Klán, P., Lefer, B., McConnell, J., Plane, J., Sander, R., Savarino, J., Shepson, P.B., Simpson, W.R., Sodeau, J.R., von Glasow, R., Weller, R., Wolff, E.W., Zhu, T., 2007. An overview of snow photochemistry: evidence, mechanisms and impacts. Atmos. Chem. Phys. 7, 4329–4373. DOI: 10.5194/acp-7-4329-2007.

Gregg, S.J., Sing, K.S.W., 1982. Adsorption, surface area and porosity. Academic Press, London. DOI:10.1002/bbpc.19820861019.

Homyak, P.M., Blankinship, J.C., Marchus, K., Lucero, D.M., Sickman, J.O., Schimel, J.P., 2016. Aridity and plant uptake interact to make dryland soils hotspots for nitric oxide (NO) emissions. Proc. Natl. Acad. Sci. USA 113, 2608–2616. DOI: 10.1073/pnas.1520496113.

Hutchinson, G.L., Vigil, M.F., Doran, J., Kessavalou, A., 1997. Coarse-scale soil–atmosphere NOx exchange modeling: Status and limitations. Nutr. Cycl. Agroecosys. 48, 25–35. DOI:10.1023/A:1009753810675.

Katagi, T., 2004. Photodegradation of pesticides on plant and soil surfaces. Rev. Environ. Contam. T182, 1–78. DOI: 10.1007/978-1-4419-9098-3.

Keeney, D.R., Hatfield, J.L., 2008. The Nitrogen Cycle, Historical Perspective, and Current and Potential Future Concerns. In: Nitrogen in the Environment: Sources, Problems, and Management (Eds. J.L. Hatfield, R.F. Follett) Academic Press, London. pp. 1–18.262. http://digitalcommons.unl.edu/usdaarsfacpub/262.

Lu, A., Li, Y., Ding, H., Xu, X., Li, Y., Ren, G., Liang, J., Liu, Y., Hong, H., Chen, N., Chu, S., Liu, F., Li, Y., Wang, H., Ding, C., Wang, C., Lai, Y., Liu, J., Dick, J., Liu, K., Hochella Jr., M.F., 2019. Photoelectric conversion on Earth's surface via widespread Fe- and Mn-mineral coatings. Proc. Natl. Acad. Sci. USA 116, 9741–9746. DOI: 10.1073/pnas.1902473116.

Ludwig, J., Meixner, F.X., Vogel, B., Forstner, J., 2001. Soil-Air Exchange of Nitric Oxide: An Overview of Processes, Environmental Factors, and Modeling Studies. Biogeochemistry 52, 225–257. DOI: 10.1023/A:1006424330555.

Manahan, S.E., 2009. Environmental Chemistry, CRC Press, Boca Raton. DOI: 10.1002/ep.670210206.

McCalley, C.K., Sparks, J.P., 2009. Abiotic Gas Formation Drives Nitrogen Loss from a Desert Ecosystem. Science 326, 837–840. DOI: 10.1126/science.1178984.

Medford, A J., Hatzell, M.C., 2017. Photon-Driven Nitrogen Fixation: Current Progress, Thermodynamic Considerations, and Future Outlook. ACS Catal. 7, 2624–2643. DOI: 10.1021/acscatal.7b00439.

Medinets, S., Skiba, U., Rennenberg, H., 2015. A review of soil NO transformation: associated processes and possible physiological significance on organisms. Soil Biol. Biochem. 80, 92–117. DOI: 10.1016/j.soilbio.2014.09.025.

509 Miranda, K.M., Espey, M.G., Wink, D.A., 2001. A rapid, simple spectrophotometric method for
510 simultaneous detection of nitrate and nitrite. Nitric Oxide 5, 62–71. DOI:
511 10.1006/niox.2000.0319.

512 Mulvaney, R.L., 1996. Nitrogen - inorganic forms. In: Methods of Soil Analysis. Part 3.
513 Chemical Methods (Ed. D.L. Sparks) American Society of Agronomy, Soil Science Society
514 of America, Madison. pp 1123–1184. DOI:10.2136/sssabookser5.3.c38.

515 Nanayakkara, C.E., Jayaweera, P.M., Rubasinghege, G., Baltrusaitis, J., Grassian, V.H., 2014.
516 Surface photochemistry of adsorbed nitrate: The role of adsorbed water in the formation of
517 reduced nitrogen species on α-Fe_2O_3 particle surfaces. J. Phys. Chem. A 118, 158–166. DOI:
518 10.1021/jp409017m.

519 Ndour, M., Conchon, P., D'Anna, B., Ka, O., George, C., 2009. Photochemistry of mineral dust
520 surface as a potential atmospheric renoxification process. Geophys. Res. Lett. 36, 224–227.
521 DOI: 10.1029/2008GL036662.

522 Nelson, D.W., Sommers, L.E., 1982. Total carbon, organic carbon, and organic matter. In:
523 Methods of soil analysis. Part 2. Chemical and microbiological properties, (Eds. A.L. Page,
524 R.H. Miller, D.R. Keeney). American Society of Agronomy, Soil Science Society of America,
525 Madison. pp. 539–579. DOI: 10.2134/agronmonogr9.2.c38.

526 Pilegaard, K., 2013. Processes regulating nitric oxide emissions from soils. Philos. Trans. Royal
527 Soc. B368. DOI:10.1098/rstb.2013.0126.

528 Sanz-Cobena, A., Lassaletta, L., Prado, A., Garniere, J., Billene, G., Iglesias, A., Sánchez, B.,
529 Guardia, G., Ábalos, D., Plaza-Bonilla, D., Puigdueta-Bartolomé, I., Morali, R., Galán, E.,
530 Arriaga, H., Merino, P., Infante-Amate, J., Meijide, A., Pardo, G., Álvaro-Fuentes, J.,
531 Gilsanz, C., Báez, D., Doltra, J., González-Ubierna, S., Cayuela, M.L., Menéndez, S., Díaz-

Pinés, E., Le-Noë, J., Quemada, M., Estellés, F., Calvet, S., van Grinsven, H.J.M., Westhoek, H., Sanz, M.J., Gimeno, B.S., Vallejo, A., Smith, P., 2017. Strategies for greenhouse gas emissions mitigation in Mediterranean agriculture: A review. Agr. Ecosyst. Environ. 238, 5–24. DOI: 10.1016/j.agee.2016.09.038.

Stern, J.C., Sutter, B., Freissinet, C., Navarro-González, R., McKay, C.P., Archer, Jr., P.D., Buch, A., Brunner, A.E., Coll, P., Eigenbrode, J.L., Fairen, A.G., Franz, H.B., Glavin, D.P., Kashyap, S., McAdam, A.C., Ming, D.W., Steele, A., Szopa, C., Wray, J.J., Martín-Torres, F.J., Zorzano, M.P., Conrad, P.G., Mahaffy, P.R., MSL Science Team, 2015. Evidence for indigenous nitrogen in sedimentary and aeolian deposits from the Curiosity rover investigations at Gale crater, Mars. Proc. Natl. Acad. Sci. USA 112, 4245–4250. DOI: 10.1073/pnas.1420932112.

Sugráñez, R., Balbuena, J., Cruz-Yusta, M., Martín, F., Morales, J., Sánchez, L., 2015. Efficient behaviour of hematite towards the photocatalytic degradation of NOx gases. Appl. Catal. B: Environ. 165, 529–536. DOI:10.1016/j.apcatb.2014.10.025.

Torrent, J., Barrón, V., 2008. Diffuse reflectance spectroscopy. In: Methods of soil analysis. Part 5. Mineralogical methods (Eds. A.L. Ulery, L.R., Drees) American Society of Agronomy, Soil Science Society of America, Madison. pp 367–385. DOI:10.2136/sssabookser5.5.c13.

Whiting, L.D., Allardice, W.R., 1986. X-Ray Diffraction Techniques. In: Methods of soil analysis. Part 1. Physical and mineralogical methods (Ed. A. Klute) American Society of Agronomy, Soil Science Society of America, Madison. pp 331–362. DOI: 10.2136/sssabookser5.1.2ed.c12.

Yao, Z., Zheng, X., Wang, R., Liu, C., Lin, S., Butterbach-Bahl, K., 2019. Benefits of integrated nutrient management on N_2O and NO mitigations in water-saving ground cover rice

production systems. Sci Total Environ. 646, 1155–1163. DOI: 10.1016/j.scitotenv.2018.07.393.

Yuan, S.J., Chen, J.J., Lin, W.W., Sheng, G.P.,Yu, H.Q., 2013. Nitrate formation from atmospheric nitrogen and oxygen photocatalysed by nano-sized titanium dioxide. Nat. Commun., 4, 2249. DOI:10.1038/ncomms3249.

Yuan, Y., Wang, Y., Ding, W., Li, J., Wu, F., 2016. Solid surface photochemistry of montmorillonite: mechanisms for the arsenite oxidation under UV-A irradiation. Environ. Sci. Pollut. R 23, 1035–1043. DOI: 10.1007/s11356-015-5017-2.

Figure captions

Fig. 1. Photochemical fixation (*ARE, FLU, FER* and *CAL*) and emission (CAM and AND) of NOx in soils. For *ARE, FLU, FER* and *CAL* soils, the concentrations of NO gas (blue line) flowing through the soil decreased abruptly when artificial sunlight was switched on at min. 10. Then, for the next 180 min under irradiation, NO gas was seemingly oxidized to NO_2, but the small increase from background levels suggests that NO_2 (black line) was in turn transformed into NO_3^-. ΣNOx ($NO+NO_2$, red line), which represents the amount converted during the experiment (yellow area), increased from the quartzitic sandy soil (*ARE*) to the calcareous clayey soil (*CAL*). In contrast, for the *CAM* and *AND* soils a NO emission (with a negative net ΣNOx, blue area) occurred, probably by photodegradation of their relatively large amounts of soluble nitrates.

Fig.2. Cumulative amounts of fixed or emitted NOx in the six soils. NO fixation (positive ΣNOx) was observed on the *ARE, FLU, FER* and *CAL* soils for natural (N), organic matter free (O) and washed (W) samples. For the *CAM* and *AND* soils, fixation only occurred for the later treatments (O and W). These soils (*CAM* and *AND*) exhibited high NO emission (negative ΣNOx) in the natural (N) treatment and for the control (C, only with air) treatment. A low NO emission was also observed for the first soils (*ARE, FLU, FER* and *CAL*). For each soil different letters denote significant differences between treatments (LSD test, $p<0.05$). The error bars indicate the standard error (three measurements).

598 Fig. 3. Effect of initial NO concentration and light intensity on the NO fixation. A) A lower
599 initial NO concentration led to higher NO conversion percentage for two representative soil
600 samples (*CAL* and *FLU*). For each soil different letters denote significant differences between
601 treatments (LSD test, $p<0.05$). B) Slight but nonsignificant differences were observed for the
602 *CAL* and FLU soils comparing the NO conversion at three light intensities. The bars indicate the
603 standard error (three measurements).

604

605

606 Fig. 4. The new N cycle in soils. Black arrows represent the classical, well-known mechanisms:
607 (A) gases (NH_3, NO, N_2O,and N_2) are released to the atmosphere by nitrification or
608 denitrification and are also produced by industrial and biological N_2 fixation, (B) gains as
609 organic N from crops and animal residues, (C) transformations among N forms ($N_{organic}$, NH_4^+,
610 NO_2^-, NO_3^- or N gases), and (D) losses from water and wind erosion, fires and leaching. Red
611 arrows complete this complex N cycle introducing the photochemical reactions affecting organic
612 matter (especially soluble organic matter, SON), NO gas and nitrates.

613

Table
Click here to download Table: Table 1-2.docx

Table 1. Composition, particle size distribution and surface area of the selected soils.

	Mineral composition (%)												
	Quartz	Feldspar	Mica	Illite	Vermiculite	Kaolinite	Smectite	Amorphous Silicates	Gibbsite	Hematite	Goethite	TiO_2	Calcite
ARE	99	0	0	0.0	0.0	0.0	0.0	-	0.0	0.0	0.1	0.1	0.0
FLU	35	14	5	16.0	0.2	0.8	0.0	-	0.0	0.2	0.5	0.3	25.0
FER	26	0	0	0.0	0.0	30.0	0.0	-	5.0	28.0	4.0	4.0	0.0
CAL	15	3	0	11.0	0.0	1.8	4.0	-	0.0	0.1	0.2	0.2	60.0
CAM	56	24	5	8.6	2.5	1.0	0.0	-	0.0	0.0	0.5	0.2	0.0
AND	20	30	0	0.0	0.0	0.0	0.0	19.0	0.0	0.0	2.8	0.7	0.6

Table 1 cont. Composition, particle size distribution and surface area of the selected soils.

	Particle size distribution (%)			Surface Area ($m^2\ g^{-1}$)	Microporosity (%)	pH	Organic Matter (%)	N forms (mg/kg)		
	Sand	Silt	Clay					NH_4^+	NO_3^-	Soluble organic N
ARE	100	0	0	0.3	0.0	8.8	0.03	1.60	0.01	4.2
FLU	55	28	17	17.3	19.7	8.7	1.20	21.60	9.80	20.5
FER	19	14	67	38.5	0.0	5.2	1.41	3.70	1.25	14.5
CAL	20	50	30	14.8	59.5	8.4	1.43	3.40	1.40	16.8
CAM	86	2	12	1.3	0.0	6.5	2.06	3.40	56.20	5.2
AND	58	36	6	21.8	13.2	5.7	8.26	0.60	31.90	1.4

Table 2. Balance of the transformation from NOx to NO_3^- for the W and O treatments

		NO_3^-		
Soil	**ΣNOx**	**Estimated**	**Measured**	**Measured / estimated**
	ppb x min	mg/kg		
ARE-W	1267	0.21	1.7	8.1
FLU-W	5324	0.88	8.5	9.6
FER-W	4195	0.7	4.6	6.5
CAL-W	4296	0.71	8.7	12.1
CAM-W	4117	0.68	7.9	11.6
AND-W	4692	0.78	16.5	21.2
ARE-O	1893	0.31	3.2	10.2
FLU-O	4665	0.77	6.4	8.2
FER-O	4739	0.79	5.1	6.4
CAL-O	5632	0.93	8.7	9.3
CAM-O	2575	0.43	3.2	7.5
AND-O	2829	0.47	11.8	25.1

Figure

Click here to download Figure: FIGURES.pdf

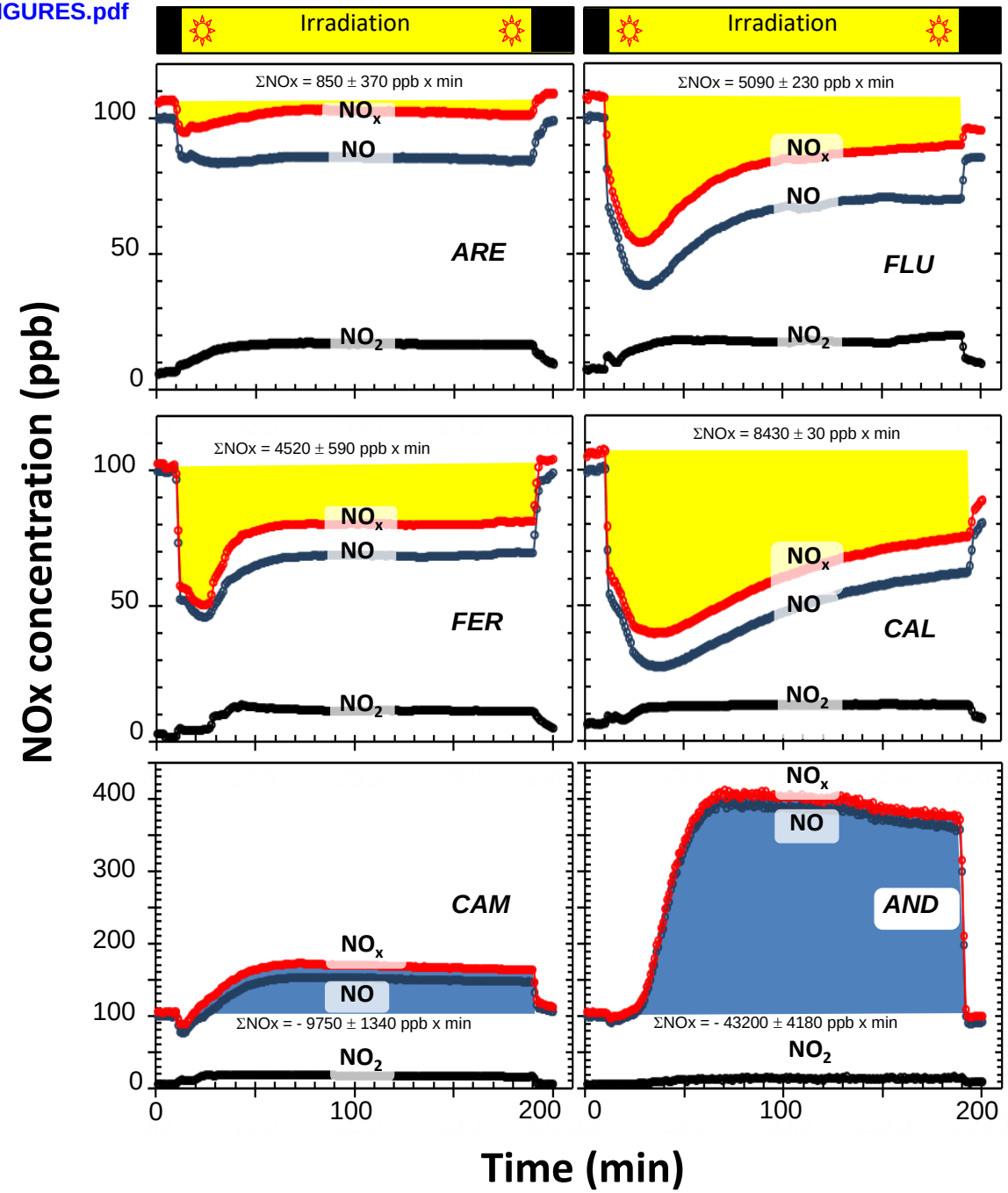

Fig.1

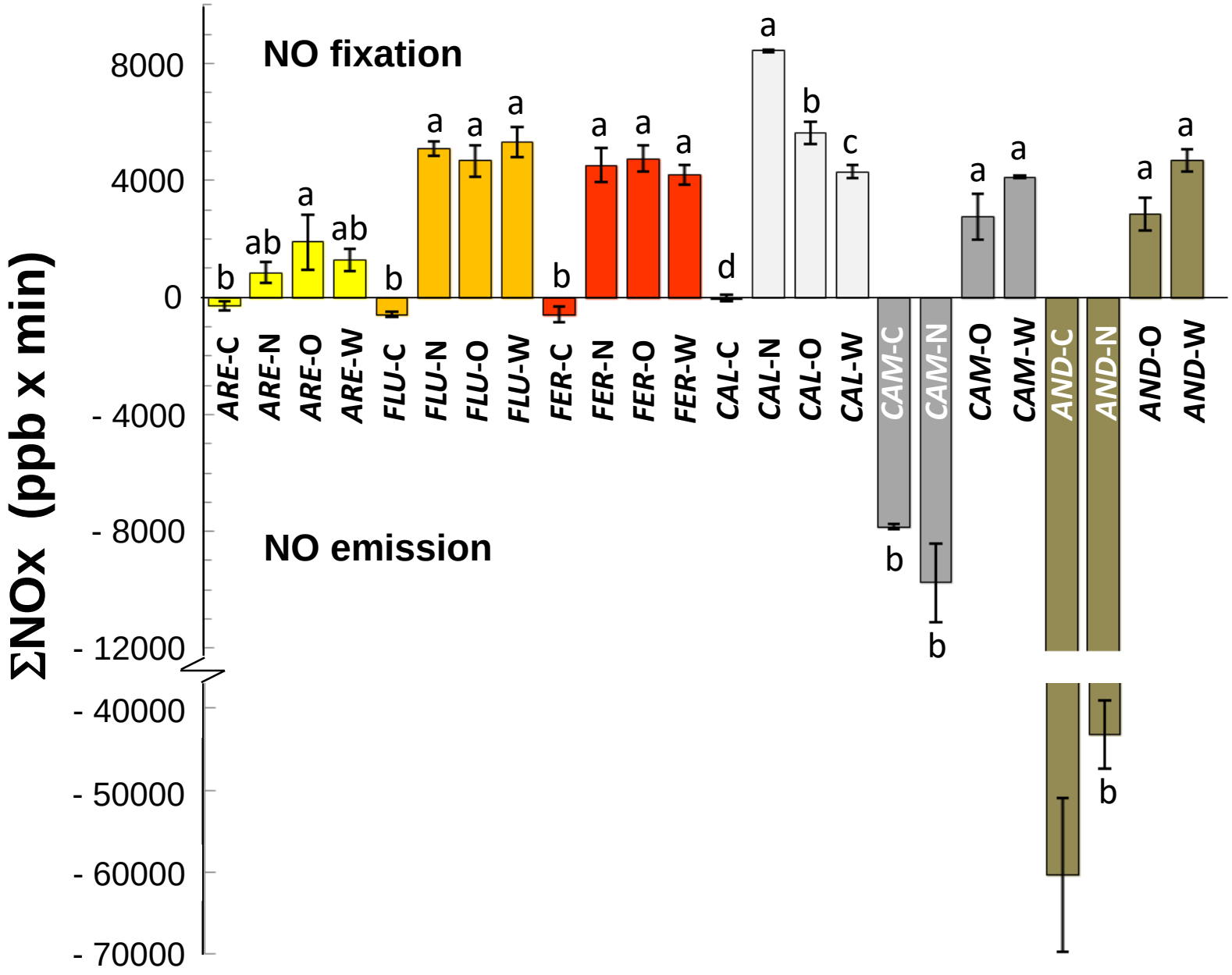
ΣNOx (ppb x min)
NO fixation
NO emission
8000
4000
0
- 4000
- 8000
- 12000
- 40000
- 50000
- 60000
- 70000
ARE-C
ARE-N
ARE-O
ARE-W
FLU-C
FLU-N
FLU-O
FLU-W
FER-C
FER-N
FER-O
FER-W
CAL-C
CAL-N
CAL-O
CAL-W
CAM-C
CAM-N
CAM-O
CAM-W
AND-C
AND-N
AND-O
AND-W

Fig.2

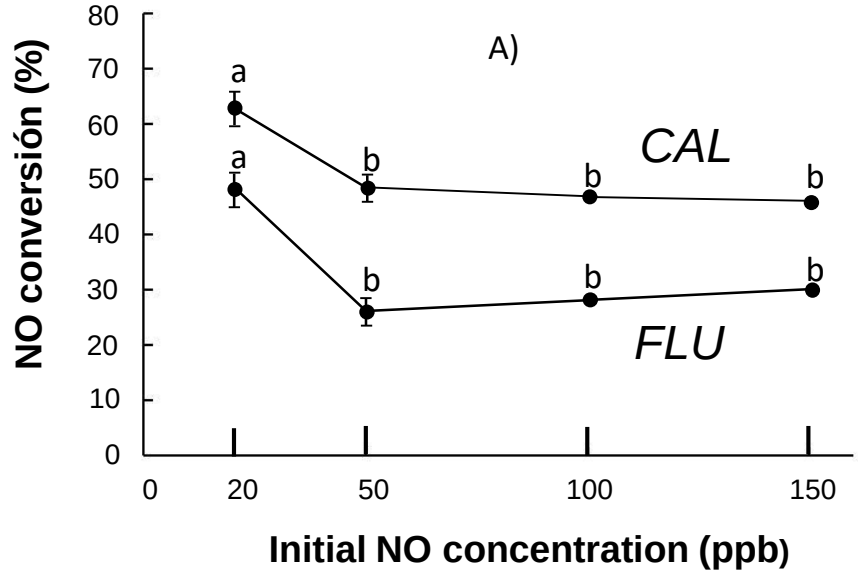
A)
NO conversión (%)
80
70
60
50
40
30
20
10
0
a
a
b
b
b
b
b
b
CAL
FLU
0
20
50
100
150
Initial NO concentration (ppb)

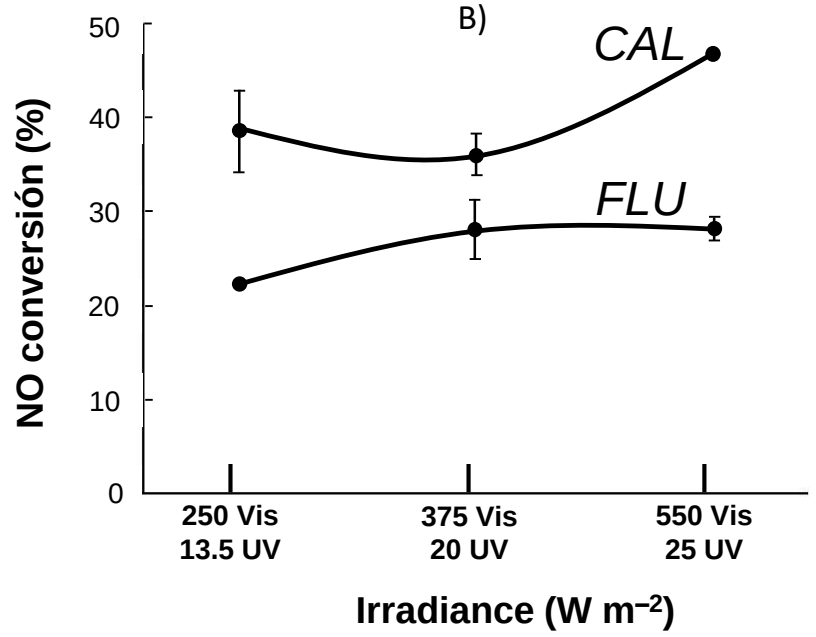
B)
NO conversión (%)
50
40
30
20
10
0
CAL
FLU
250 Vis
13.5 UV
375 Vis
20 UV
550 Vis
25 UV
Irradiance (W m⁻²)

Fig.3

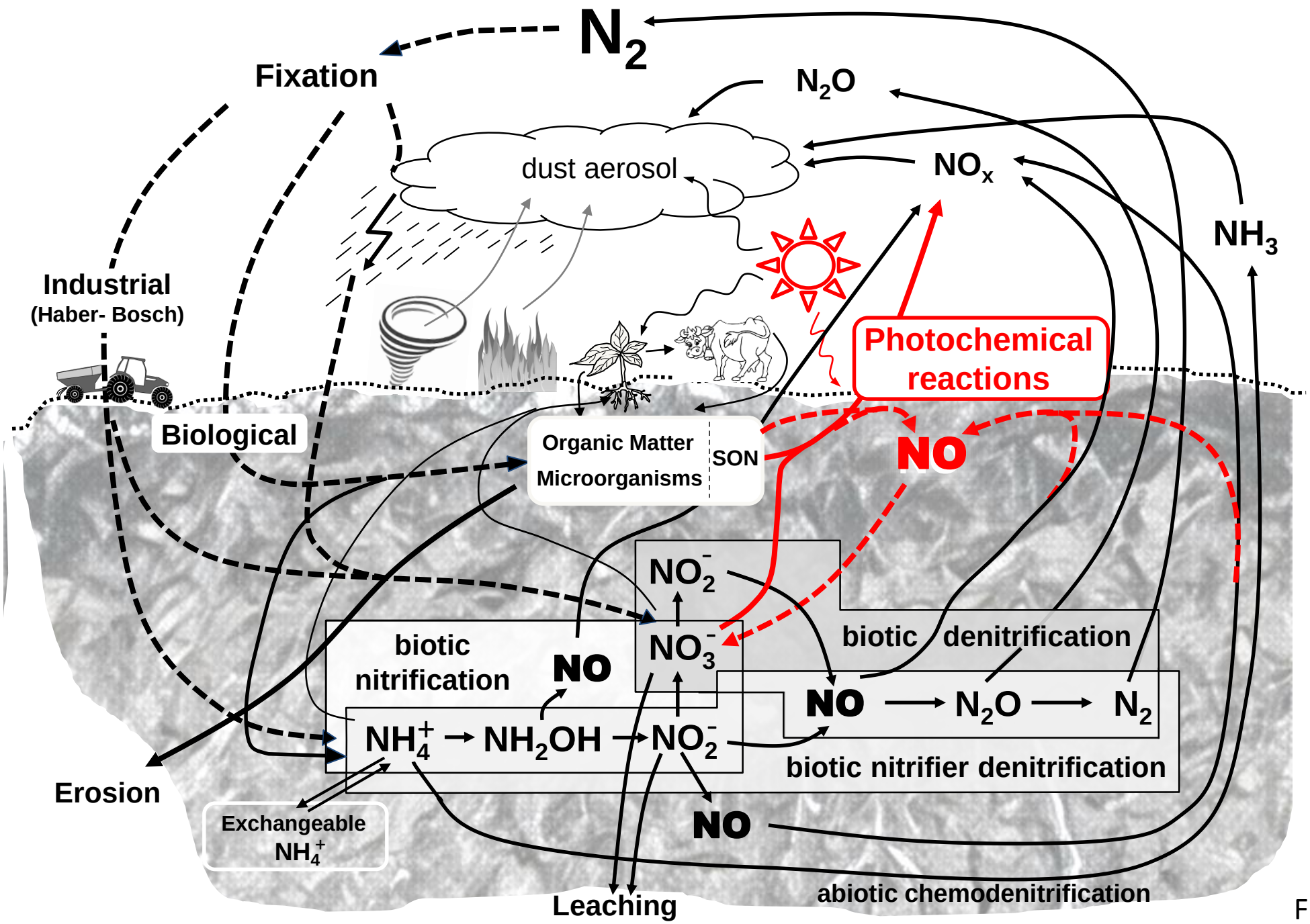
N_2
Fixation
N_2O
dust aerosol
NO_x
NH_3
Industrial
(Haber- Bosch)
Photochemical
reactions
Biological
Organic Matter
Microorganisms
SON
NO
NO_2^-
NO_3^-
biotic
nitrification
NO
biotic denitrification
NO → N_2O → N_2
NH_4^+ → NH_2OH → NO_2^-
biotic nitrifier denitrification
Erosion
Exchangeable
NH_4^+
NO
Leaching
abiotic chemodenitrification

Fig.4